International Journal of Biological Macromolecules 152 (2020) 1194–1204

Contents lists available at ScienceDirect

International Journal of Biological Macromolecules

journal homepage: www.elsevier.com/locate/ijbiomac

The effect of biomimetic coating and cuttlebone microparticle reinforcement on the osteoconductive properties of cellulose-based scaffolds

Alisa Palaveniene [a], Kristina Songailiene [a], Odeta Baniukaitiene [a], Sedef Tamburaci [b], Ceren Kimna [b], Funda Tihminlioğlu [b,*], Jolanta Liesiene [a]

[a] Department of Polymer Chemistry and Technology, Kaunas University of Technology, Lithuania
[b] Department of Chemical Engineering, Izmir Institute of Technology, Turkey

ARTICLE INFO

Article history:
Received 16 May 2019
Received in revised form 9 October 2019
Accepted 24 October 2019
Available online 20 November 2019

Keywords:
Cuttlebone
Bone scaffold
Biomimetic
Simulated body fluid
Osteoconductive

ABSTRACT

Polymer-based scaffolds have already gained popularity in many biomedical applications due to convenient routes for fabrication and favourable structural, physicochemical and functional characteristics. However, polymeric scaffolds lack osteoconductivity and some synthetic polymers carry the risk of inflammatory response caused by degradation by-products. Those facts limit their practical use in bone tissue engineering. In this study, three-dimensional (3D) porous scaffolds from naturally derived polymer, namely regenerated cellulose, were prepared using a non-hydrolytic sol-gel and lyophilization techniques. To induce osteoconductive properties of the polymeric scaffolds, cuttlebone microparticles were immobilized and the surface coating was achieved via *in vitro* mineralization using 10-fold concentrated simulated body fluid (10x SBF). Biogenic activity of cuttlebone is explained by its chemical composition, which includes polysaccharide *β*-chitin and macro-, micro- and trace elements favourable for mineralization. Parallel the scaffolds were examined during long-term (24 weeks) *in vitro* mineralization in 1x SBF for the purpose to investigate apatite-forming ability of the scaffolds. A nice cauliflower-like structures and needle-like dents of the spherical aggregates, which are characteristic to hydroxyapatite precursors, were observed on the surface of cellulose/cuttlebone scaffolds by SEM. 10x SBF coating enhanced cell attachment to the scaffolds because SBF elements are known to increase bioactivity by inducing re-deposition of carbonate apatite crystallites on scaffold surface. Additionally, calcium and phosphate depositions were clearly observed on the developed scaffolds using von Kossa and Alizarin Red S staining. Proliferative and osteoconductive effects on the osteoblast-like MG-63 cells demonstrate the cellulose/cuttlebone scaffolds soaked in 10x SBF as a favourable material for bone tissue engineering.

1. Introduction

Cuttlebone is of great interest for bone tissue engineering as a bioactive mineral filler because it contains biogenic calcium and bioinorganic trace elements. Several studies have shown high levels of cuttlebone osteoconductivity, bioactivity, and chemical and structural conformity towards human bone tissue. Dogan and Okumus [1] showed that the small pieces of crushed cuttlebone used for xenogeneic grafts promote the healing of bone defects *in vivo*. Kim et al. [2] compared the bioactivity of cuttlebone-derived hydroxyapatite (HAp) and synthetic HAp granules. After 7 days, the cells cultured on cuttlebone-HAp granules had almost 2-fold higher ALP activity compared to their activity on synthetic HAp granules. Therefore, biogenic calcium of marine origin, specifically from cuttlebone, could be substantially helpful for developing bioactive and biocompatible bone grafts.

Recently, implantation of bone grafts has become fairly common in routine clinical practice. Notably, ongoing research in the field of bone tissue engineering is focused on the development of biomimetic bone scaffolds. 3D polymer-based porous scaffolds are frequently chosen as a multifunctional materials to reconstruct cancellous bone structure. However, the bioinert surface of polymer matrices argues against the bioactivity of these materials [3]. To enhance the osteoconductive properties of polymeric scaffolds, composites with calcium minerals are usually prepared. This enhancement is usually achieved by (i) using biomimetic coating and/or (ii) preparing polymer/inorganic blends.

* Corresponding author.
E-mail address: fundatihminlioglu@iyte.edu.tr (F. Tihminlioğlu).

https://doi.org/10.1016/j.ijbiomac.2019.10.213
0141-8130/

Biomimetic coating, otherwise *in vitro* mineralization, has become a conventional route for the formation of HAp ($Ca_{10}(PO_4)_6(OH)_2$) layer on a surface of modified polymeric scaffolds. Before *in vitro* mineralization, polymer-based scaffolds are modified by introducing specific functional groups, such as hydroxyl, carboxyl, phosphate, and silanol groups [4]. Coating of polymer surfaces with calcium minerals can be achieved by using different techniques, for example, soaking in simulated body fluid (SBF), slurry dipping or electrophoretic deposition and thermally sprayed calcium phosphate droplets [5,6]. Some novel interpretations of the existing techniques have been recently published. Abdal-hay et al. [7] developed *in situ* biomineralization and subsequent freeze-drying to prepare a highly porous bioactive chitosan-based 3D scaffold. Douglas et al. [8] revealed the impact of enzymatic mineralization on osteoblastic MC3T3-E1 cell activity and showed the viability of gellan gum hydrogel composites.

In the literature, SBF coating is a common technique to improve osteoconduction of biomaterials for hard tissue engineering applications. Numerous studies demonstrate that calcium phosphate-incorporated biomimetic coating improves the osteoconductive properties of polymer-based scaffolds. He et al. [9] demonstrated that poly(lactic acid) fibrous matrices facilitate the proliferation and differentiation of preosteoblastic cells (MC-3T3-E1) when pre-incubated in SBF. Lee et al. [10] also demonstrated that biomimetic coating with a silk nanofiber surface by immersion in 10x SBF markedly improved osteoblast adhesion and proliferation. Aday and Gumusderelioglu [11] fabricated porous chitosan scaffolds that were immersed in 10x SBF and confirmed that SBF treatment increased the calcium deposition compared to untreated scaffolds. In a study by Kong et al. [12], chitosan/nano-HAp composite scaffolds were coated with 5x SBF to enhance bioactivity of the scaffolds.

Samaneh Saber-Samandari et al. [13] prepared cellulose-graft-polyacrylamide/nano-hydroxyapatite nanocomposite scaffolds by using free radical polymerization and freeze-drying technique. The authors investigated apatite-forming ability by soaking the scaffolds in 1x SBF for 28 days. Lyophilization, otherwise freeze-drying, is used to improve stability of polymeric nanoparticles [14] or to achieve porous structure of scaffolds for bone tissue engineering. With regard to natural polymers, cellulose, alginate or chitosan, etc. [13,15,16] are usually used as a base matrix for the developing of porous freeze-dried scaffolds.

In this study, 3D scaffolds were prepared using a non-hydrolytic sol-gel technique from regenerated cellulose and mechanically immobilized cuttlebone microparticles. Regenerated cellulose was chosen as a scaffold matrix as a biocompatible and naturally-derived biomaterial. The porous structure of the scaffolds was achieved by lyophilization. To enhance the osteoconductive properties of the scaffolds, the surface coating was performed via *in vitro* mineralization using 10x SBF. The impacts of the cuttlebone and biomimetic coating of the scaffold surface on the osteoconductive properties of cellulose-based composite scaffolds were examined using osteoblast-like MG-63 cells as an *in vitro* cell culture model.

2. Materials and methods

2.1. Materials

Cuttlebones were purchased from Vital Pet Products Ltd, UK. Cellulose acetate (Mn ~ 50,000) and sodium dodecyl sulfate (SDS) were obtained from Sigma-Aldrich. All reagents for 1x and 10x SBF were reagent grade (Eurochemicals). Minimum Essential Medium Eagle (MEM, Sigma-Aldrich), fetal bovine serum (FBS-Lonza) penicillin-streptomycin solution and L-glutamine (Lonza) were used for the cell culture experiments. Silver nitrate (Sigma-Aldrich) and sodium thiosulfate (Sigma-Aldrich) were used for the von Kossa staining. WST-1 cell viability kit (BioVision Inc.), Lactate dehydrogenase (LDH) assay (Thermo Fisher Scientific) and the ALP-Enzyline PAL optimise kit (Biomerieux Inc.) were used for *in vitro* studies. L-ascorbic acid (Sigma-Aldrich) and *β*-glycerophosphate (Sigma-Aldrich) were used for osteogenic medium preparation. Alizarin Red S (Sigma-Aldrich) was used for the Alizarin Red S staining protocol. DAPI and Alexa Fluor 555 (Thermo Fisher Scientific Inc.) stains were used for fluorescence imaging.

2.2. Cuttlebone microparticles

2.2.1. Preparation of cuttlebone microparticles

Cuttlebone pieces were ground in an agate mortar, sieved, and a fraction of microparticles 35–42 μm was collected. The powdered material was washed to remove proteins under continuous stirring for 1 h and heating at 80 °C with 0.5 M NaOH solution and further with 1% SDS solution in a 1:4 ratio (w/v). After deproteinization was complete, the cuttlebone microparticles were thoroughly washed with distilled water and dried. The effectiveness of SDS removal from the material was checked by adding 1% $BaCl_2$ solution to the washing solution (white precipitate in positive result), because SDS is a source of SO_4^{2-} ions.

2.2.2. Characterization of cuttlebone microparticles

Elemental composition, morphology and chemical structure of cuttlebone particles were investigated in our previous study by using XRF, SEM and FT-IR analyses [17].

In this study, lamellar and dorsal segments of cuttlebone were analysed by thermogravimetric (TGA) analysis. Lamellar and dorsal parts were carefully separated by using a scalpel; both parts were ground separately in an agate mortar and sieved. Powdered cuttlebone was then dried in an oven at 100 °C temperature for 1 h and stored in a desiccator until an analysis. Ten (10) mg of a sample were placed in a platinum pan and heated up to 900 °C temperature under oxygen atmosphere at a heating rate of 10 °C/min (Perkin Elmer TGA 4000 analyser). Particle size distribution in the prepared samples (n = 3) was determined by laser particle sizer (Fritsch analysette 22 Nano Tech) covering a size range of 0.01–2 100 μm. Liquid dispersion method (by means of ultrasound application for 5 min) was used to disperse agglomerates.

2.3. Preparation of cellulose-based scaffolds with cuttlebone microparticles

For the preparation of composite scaffolds, cuttlebone microparticles were mechanically immobilized within the RC gel using a technique as described in our previous study [18], where synthetic HAp was used as a filler. The porous structure of the scaffolds was achieved by lyophilization in a Christ Alpha 2–4 LSC lyophilizator. Three groups of cellulose-based scaffolds were prepared: 1) an RC/CB scaffold; 2) an RC/CB-SBF scaffold additionally soaked in 10x SBF as described in the literature [10]; and 3) an RC scaffold without any filler or coating as a control. Cylindrical samples (1.0 × 1.5 ± 0.2 cm) were prepared for further experiments.

2.4. Apatite-forming ability of the scaffolds

2.4.1. Soaking of RC-based scaffolds in 1x SBF

Samples were immersed in 1x SBF for up to 24 weeks. 1x SBF was prepared by a method and the recommendations of Kokubo et al. [19]. Briefly, calculated amounts of chemical reagents were added to distilled water and buffered with a solution of Tris/HCl and 1.0 M HCl up to pH 7.4. The samples were immersed in the

solution and kept in an incubator shaker at 37 °C and 120 rpm speed for particular periods of time; the medium was changed every 2 weeks by the freshly prepared one. Scaffold samples were removed from the solution every 2 weeks, rinsed with distilled water and dried in an oven at 40 °C until constant weight.

2.4.2. Characterization of the scaffolds during soaking in 1x SBF

Scaffolds were examined using FEI Quanta 200 FEG scanning electron microscopy/energy dispersive spectrum (SEM/EDX), Fourier transform infrared spectroscopy (FTIR, Perkin-Elmer, Inc., Waltham, USA) and X-ray diffraction (XRD, Bruker AXS, Karlsruhe, Germany) spectrometry analyses.

2.5. In vitro cell culture studies

Scaffolds were subjected to ethylene oxide sterilization before *in vitro* experiments. The osteoblast-like MG-63 cells were cultivated in MEM Eagle's medium supplemented with 10% fetal bovine serum (FBS), 1% L-glutamine and 1% streptomycin/penicillin at 37 °C in a humidified 5% CO_2 atmosphere.

2.5.1. In vitro cytotoxicity determination

An *in vitro* cytotoxicity assay was performed according to ISO10993-5 standards (Biological evaluation of medical devices Part 5: Tests for *in vitro* cytotoxicity). Scaffolds were incubated in cell culture medium (MEM) for 24 h at 37 °C. After incubation, scaffolds were removed, and medium was used as the extract of the scaffold. Cell seeding was carried out at a 10^5 cells/mL cell density and incubated on 96-well plates. The cytotoxicity of the samples was evaluated by incubation of cell monolayer with extraction medium and cell viability measurement. The viability of MG-63 cells was evaluated by the WST 1 assay, which was based on the conversion of stable tetrazolium to a soluble formazan occurring primarily at the cell surface [20]. The cytotoxicity of the sample extracts was evaluated with respect to the cell viability of control group (NC). Optical density of each well was measured as OD value at 440 nm. Cell viability was obtained by normalizing the OD values with respect to the control group and calculated according to Eq. (2.1):

$$\text{Cell viability}\,(\%) = (\text{Absorbance of a sample}/\text{Absorbance of NC}) \times 100 \quad (2.1)$$

where *NC* is a negative control that includes MG-63 cells incubated without sample extract.

2.5.2. Cell attachment on scaffolds

Cell attachment studies were performed using fluorescence microscopy (Zeiss Observer Z1). MG-63 cells were seeded on the scaffolds and incubated for 7 days. The cells on the scaffolds were fixed with a 3.7% paraformaldehyde (w/v in PBS) solution for 20 min at room temperature before staining. Then, samples were stained with DAPI and Alexa Fluor 555 fluorescence stains to visualize the nuclei and actin filaments of cells respectively.

2.5.3. Cell proliferation assay

Cell proliferation on the scaffolds was determined by using the WST-1 Cell Viability Kit. For proliferation assay MG-63 cells were seeded at a density of $2.5x10^6$ cells/scaffold in a 24-well plate. Cell cytotoxicity was also determined with LDH assay to investigate the cell death during incubation.

2.5.4. ALP activity

The extracellular ALP secretion was evaluated with ALP-Enzyline PAL optimise kit. The MG-63 cells were seeded at a density of 2.5×10^6 cells/scaffold and cultured with the osteogenic medium on the scaffolds for ALP activity determination. ALP activities of the cells were quantified by a colorimetric ALP kit at 7, 14, 21 and 28 days of incubation. The absorbance of the medium was measured by a plate reader (Varioskan Flash) at 405 nm.

2.5.5. Osteocalcin secretion

Osteocalcin (OC) as an important protein marker for bone tissue formation, is involved in the biomineralization process. Osteocalcin secretion of cells on scaffolds was analyzed with Sandwich ELISA (Human OC/BGP (Osteocalcin) ELISA Kit, Elabscience). The culture media extracted from scaffolds were used to detect OC production for 14 and 21 days of incubation.

2.5.6. In vitro biomineralization with von Kossa and Alizarin red staining

Von Kossa and Alizarin Red S staining were used to detect mineral formation by cells cultivated on scaffolds. After incubation, the osteogenic medium was removed, and scaffolds were washed with 1x PBS solution three times. Cell fixation was carried out with 3.7% paraformaldehyde for 20 min at room temperature and scaffolds were washed with 1x PBS solution, subsequently with distilled water several times. For von Kossa staining, each scaffold was incubated with 1% (w/v) aqueous silver nitrate solution for 30 min under UV light in a laminar flow cabinet. After incubation, silver nitrate solution was aspirated, scaffolds were rinsed with distilled water and incubated with 5% (w/v) sodium thiosulfate solution for 5 min to remove unreacted silver. Then scaffolds were washed again with distilled water. Alizarin Red S staining protocol was used to detect calcium deposition. Scaffolds were stained with 2% (w/v) aqueous alizarin red S solution by incubating the samples at room temperature in the dark for 30 min. After incubation, Alizarin Red S solution was aspirated, and scaffolds were rinsed with distilled water several times. The stained samples were observed under a stereomicroscope (Olympus SOIF DA 0737) to detect yellowish-brown and red stain for phosphate and calcium deposition respectively.

2.6. Statistical analysis

For *in vitro* cell culture studies, all experiments were repeated three times, and the experimental data were expressed as the mean ± SED. Statistical analyses of *in vitro* studies were carried out using two-way analysis of variance (ANOVA) with a Tukey's multiple comparison test. Statistical significance was indicated by $P < 0.05$.

3. Results and discussion

3.1. Characterization of cuttlebone microparticles

The cuttlebone is composed of two main structural segments: the lamellar matrix and dorsal shield. These segments are different in terms of chemical composition and morphological structure. Morphological differences were presented in our previous study [17]. According to morphology and elemental composition of cuttlebone, it is a favourable natural material for mineralization [17]. To the best of our knowledge thermogravimetric analysis (TGA) data on separated lamellar and dorsal parts of cuttlebone was not presented before. TGA results of these two structurally different parts should give more precise information about cuttlebone material as a whole.

Thermal degradation curves of cuttlebone samples are shown in Fig. 1 (a). Three-stage decomposition in TGA curves are typical for cuttlebone [21,22,23]; and were clearly observed in our study both

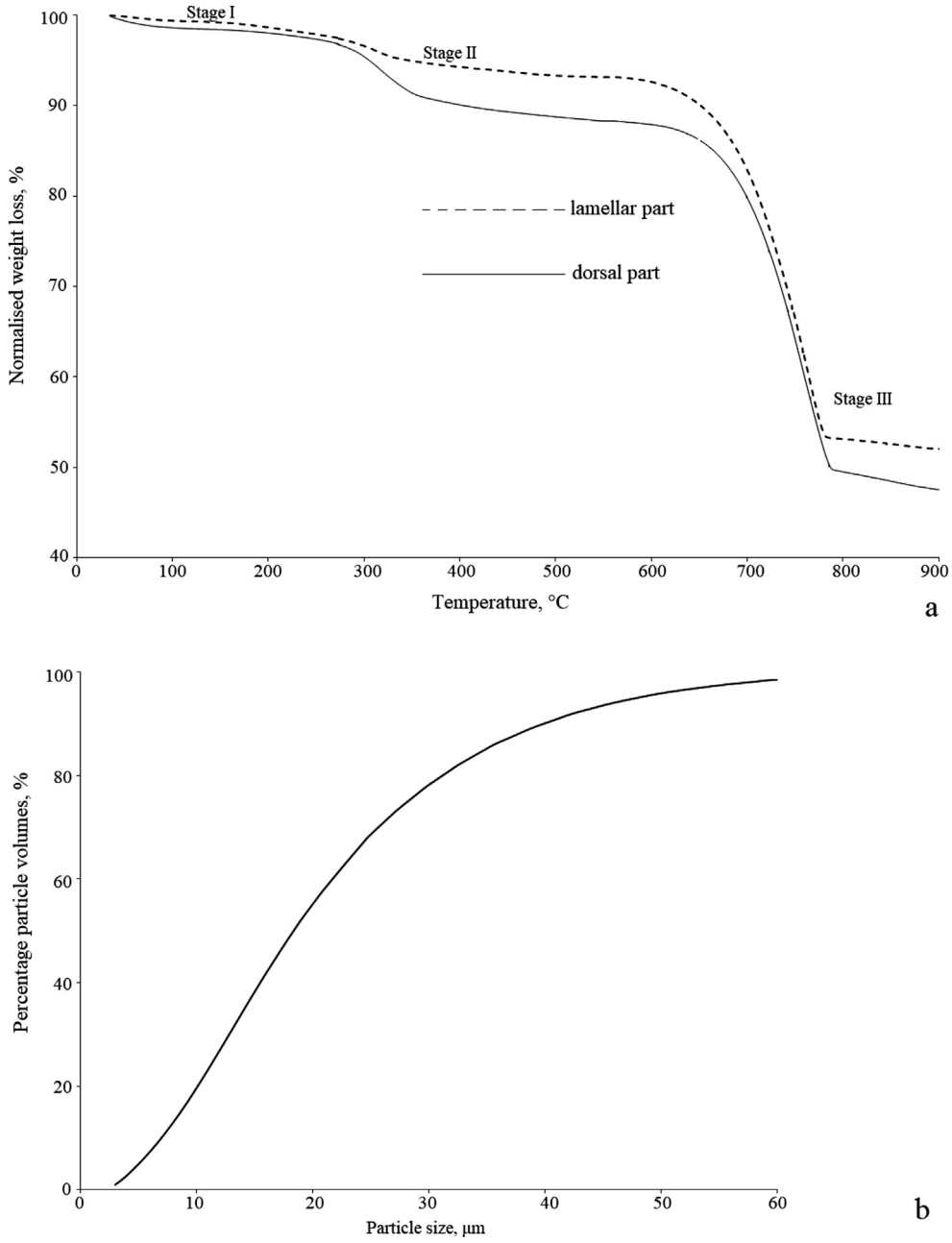

Fig. 1. Characteristics of cuttlebone microparticles: TGA curves of lamellar and dorsal parts (a); particle size distribution (b).

for lamellar and dorsal parts of cuttlebone. Stage I refers to removal of absorbed moisture at 35–100 °C temperature (approx. weight loss 1% for pre-dried samples), stage II refers to decomposition of organic matter, like polysaccharide β-chitin linked with glycoprotein and protein compounds [24] at 340–360 °C temperature; and stage III refers to aragonite (one of the crystalline polymorphs of calcium carbonate) decomposition at 780–790 °C temperature (total weight loss 46–50%) [23]. Lamellar and dorsal part samples had 5% weight loss at 345 °C and 9% at 355 °C, respectively. Results of TGA analyses showed non-equal distribution of organic matter in both lamellar and dorsal parts of cuttlebone at decomposition stage II. Almost double amount of organic matter was found in a dorsal part. These results coincide with the study done by Le Pabic et al. [24]. To sum up, predominant portion of chitin is located in the dorsal part of the cuttlebone (9% of total organic matter), whereas the framework of pillars in the lamellar part is also based on chitin (5% of total organic matter).

In the present study, powdered mixture of lamellar and dorsal parts of cuttlebone was used further. It was assumed that milling of non-separated cuttlebones should be technologically more reasonable and affordable operation for future manufacturing of cuttlebone-derived products.

Generally, obtaining optimal particle size has an impact on uniformity of a content, while content uniformity could be enhanced by decreasing particle size [25]. Powdered cuttlebone particles were sieved and fractionated (35–42 μm) before laser diffraction analysis. Analysis results showed that the particle size distribution for a micronized cuttlebone samples covered a size range from 3 μm up to 60 μm (Fig. 1 (b)). Predominant percentage (90%) of particle size was up to 40 μm. Major percentage (78%) of particles

were in a particle size<30 μm that could be explained by generally known disadvantages of laser diffraction method, namely: (a) reported distribution can be deviated towards a smaller range and (b) measurement of non-spherical particles appear in less accurate results. Only 10% of particles formed agglomerates and marginally changed their initial size up to 60 μm.

3.2. Apatite-forming ability of RC-based scaffolds during soaking in 1x SBF

Biomimetic coating *via* immersion of samples in SBF serves as a traditional and effective method for the evaluation of bioactivity *in vitro*. The formation of the HAp layer on the surface of a scaffold is usually assumed as *in vitro* bone-bonding ability of an experimental graft.

Cuttlebone incorporated RC scaffolds (RC/CB scaffolds) were already characterized in terms of morphology, chemical structure and mechanical strength by Palaveniene et al. [17], including (i) elemental composition and morphology of cuttlebone lamellar and dorsal parts, (ii) morphology of the scaffolds by micro-computed tomography, (iii) mechanical testing and (iv) specific cytotoxicity evaluation by using hepatocytes and *extensor digitorum longus* muscle cells. According to our previous results, the structure of the RC/CB scaffolds is interconnected and highly porous (porosity 80%), the pores are randomly ordered (320 μm pore size). Results of mechanical testing showed that incorporation of cuttlebone enhanced the elastic modulus and compressive strength of a cellulose matrix. Basic physical parameters of the scaffolds during soaking in SBF, such as water retention, swelling and degradation ratios and analysis of SBF solution during soaking of scaffolds are presented elsewhere [26]. In this study, cuttlebone material was further characterized (Section 3.1), deproteinized by using detergent and the RC/CB-based scaffolds were mineralized in concentrated 10x SBF to accelerate the process.

Fig. 2 shows the microphotographs of samples surface before and after 2–24 weeks of *in vitro* mineralization. The main differences in surface morphology between composite scaffolds (Fig. 2 (a)) and the cellulose matrix (Fig. 2 (d)) were observed. The surface of the RC/CB scaffold was covered with a compact layer of apatite precursor spheres even after 2 weeks of immersion in 1x SBF (Fig. 2 (b)). The number and size of apatite precursors increased, inducing the formation of aggregates on the scaffold surface (Fig. 2 (c)). The crystal size increases through crystal-crystal interactions, whereas the hydrated surface of apatite crystals promotes the process [27]. Simultaneously, the RC scaffold showed no signs of apatite precursor formation even after 24 weeks of immersion in 1x SBF (Fig. 2 (e, f)). This observation obviously confirms that the RC scaffold could not be characterized as an osteoconductive polymer. Thus, immobilization of cuttlebone bioactive material could significantly increase osteoconductive properties of the RC scaffold.

Fig. 3 shows the SEM/EDX of RC/CB scaffolds before and during soaking in 1x SBF. EDX analysis revealed the elemental composition of the RC/CB scaffolds surface before and during immersion in 1x SBF, respectively (Fig. 3 (a, b, c)). The signal from P (Fig. 3 (b, c)) confirms the formation of phosphates on the scaffold surface. Different microelements, such as Ca, Mn, Fe and Zn are characteristic of cuttlebone, whereas C and O are derived from cellulose compositional elements. Moreover, elements Mn and Zn are generally assumed as promoters of bone tissue formation by improvement of osteoblastic cell adhesion as well as growth and osteocalcin expression [28].

In addition to those factors, a cauliflower-like morphology of apatite spheres was observed on the surface of RC/CB scaffolds (Fig. 3 (e, f)). This shape is characteristic of HAp precursors, which was clearly demonstrated in the literature [29]. The needle-like dents were observed on some spherical aggregates (Fig. 3 (e)). Such morphology corresponds to the longitudinal orientation of plate-like apatite transformed from apatite precursor spheres [30].

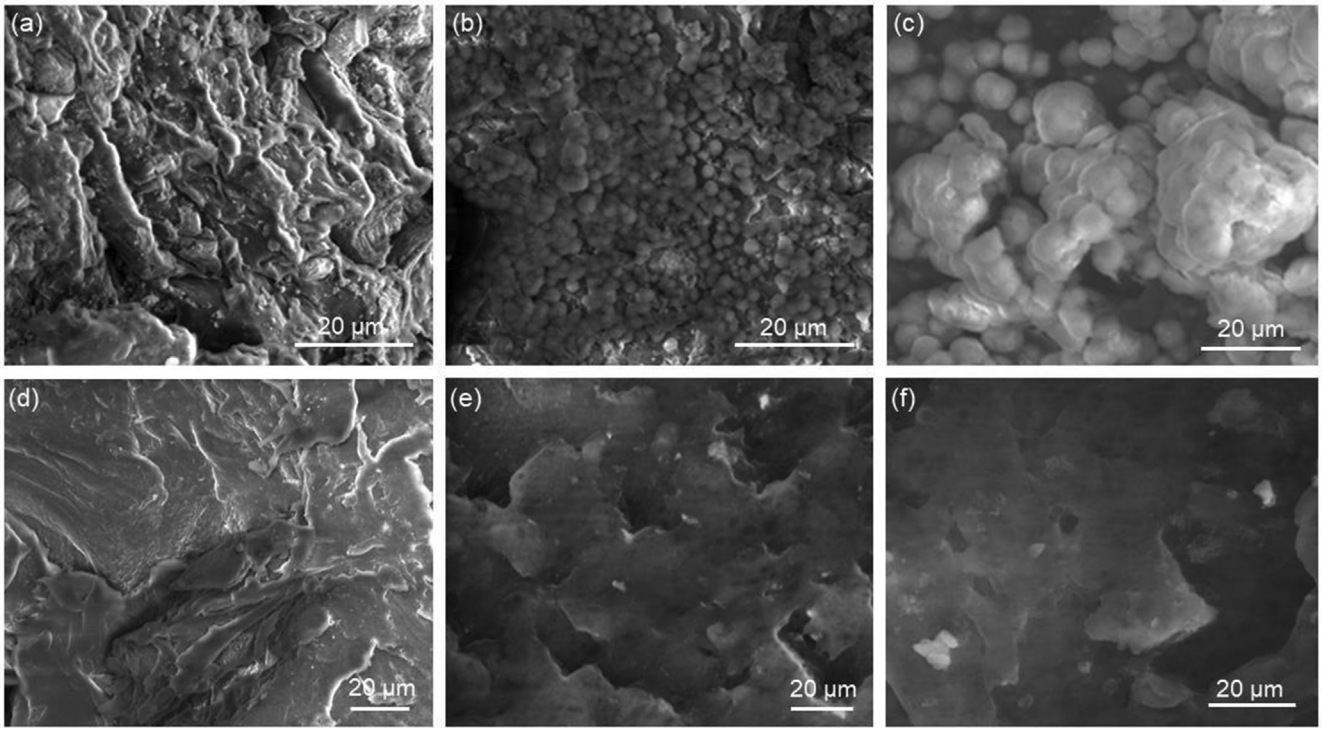

Fig. 2. SEM images of RC/CB scaffolds (a, b, c) and an RC scaffold (d, e, f) for different soaking periods (*in vitro* mineralization): before immersion, after 2 weeks of immersion and after 24 weeks of immersion in 1x SBF, respectively.

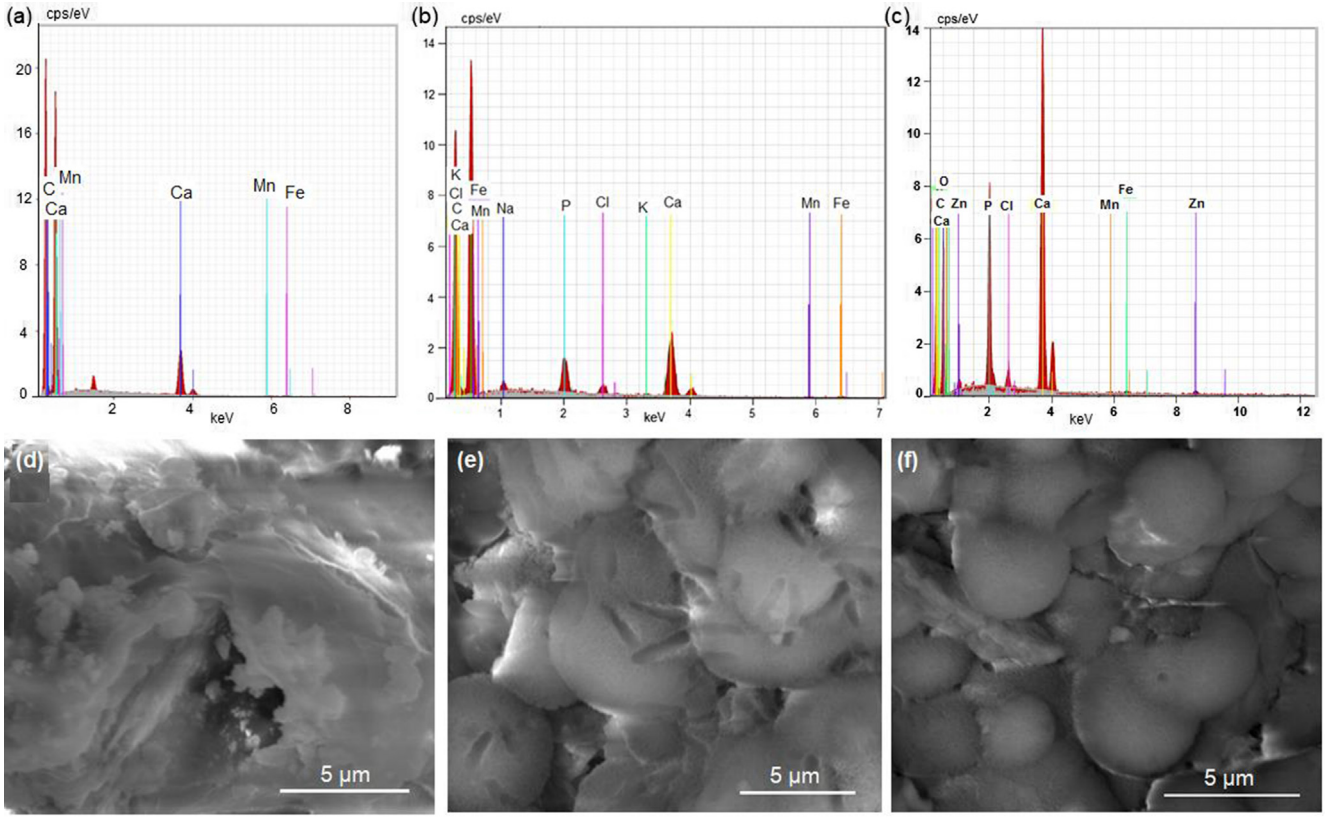

Fig. 3. EDX elemental data determined over the area of interest and SEM images of the RC/CB scaffold surface during *in vitro* mineralization: original sample, no soaking (a, d); after 2 weeks (b, e); and after 24 weeks (c, f) of soaking in 1x SBF.

The *in vitro* bioactivity of the scaffolds was assessed in terms of their ability to form apatite layer on the surface and thus to mimic physiological bone restoration process [4]. Usually SBF studies are performed up to 24 days. However, in our study, specific zoom on the time frame of 24 weeks was done. The extensive period of time of SBF study was observed because in clinical practice bone scaffolds are used to serve more than few months, usually it takes a few years.

FTIR spectra of the scaffolds before and after soaking in 1x SBF are presented in Fig. 4. Absorption peaks of PO_3^{4-} group at 604 cm^{-1} and 560 cm^{-1} [31] were observed for the RC/CB scaffolds after 5 weeks of immersion (data not shown). Absorption peaks of the phosphate group were prominently conspicuous for the RC/CB scaffolds during soaking in SBF. The RC scaffolds showed no characteristic absorption peaks of the phosphate group, even after 24 weeks of soaking in 1x SBF.

The XRD patterns of RC/CB scaffolds were identified by using a Search Match database (powder diffraction file 01–074-976). The obtained data (not shown) revealed that a low intensity of diffracted X-rays for the RC/CB scaffolds after soaking in 1x SBF are characteristic peaks of HAp at 25.4°, 31.7°, 34.1°, 39.7°, 46.7° and 49.6°. The XRD patterns of the RC/CB scaffolds after soaking in 1xSBF show that the characteristic peaks of aragonite remain. The XRD patterns at 12.3° and 20.5° are characteristic of cellulose [32]. The XRD pattern of the RC scaffold (control group) showed no presence of HAp even after 24 weeks of testing. Obtained data also confirms the impact of immobilized cuttlebone microparticles to the HAp nucleation on the surface of the cellulose-based scaffold.

According to the positive results of FTIR and XRD analyses, further cell culture experiments (Sections 3.4–3.9) were performed using express 10x SBF solution for the biomimetic coating of the RC/CB scaffolds.

3.3. Cytotoxicity determination

MG-63 cells interacted with RC/CB scaffold extracts to investigate the possible effects of cuttlebone microparticles on cell viability. High cell viability results were obtained for all groups. Scaffold extracts showed no cytotoxic effect (cell viability >50%) on MG-63 cells with 72 h of incubation (Fig. 5). The cell viability results of all cellulose-based scaffolds were found to be significant for 48 h and 72 h compared to the RC scaffold as a control group ($P < 0.05$). For 24 h of incubation, the cell viability results of the RC/CB scaffolds were found to be significantly different compared to the control group (RC scaffold) and between each other. No significant difference was observed between the groups.

Results showed that higher cell viability was obtained with an RC/CB group which was covered with 10x SBF components. It was revealed that the scaffold extracts of each group did not show any cytotoxic effect on MG-63 cell lines. In a study, Li and coworkers [33] generated cuttlebone scaffolds for bone tissue engineering applications and investigated the *in vitro* cytotoxicity of scaffold extracts. Similarly, cuttlebone extracts were found to be non-toxic (relative cell viability $\geq$100%) and showed no inhibitory effects on cell proliferation.

3.4. Cell attachment on scaffolds

Fluorescence microscopy images of MG-63 cells were obtained with DAPI nucleus stain and Alexa Fluor 555 cytoskeleton stain. Fluorescence images of MG-63 cells attached on scaffolds for 7 days are depicted in Fig. 6. The images show that cells were successfully attached to cellulose-based scaffold surfaces during incubation. Cuttlebone incorporation enhanced cell attachment on the RC

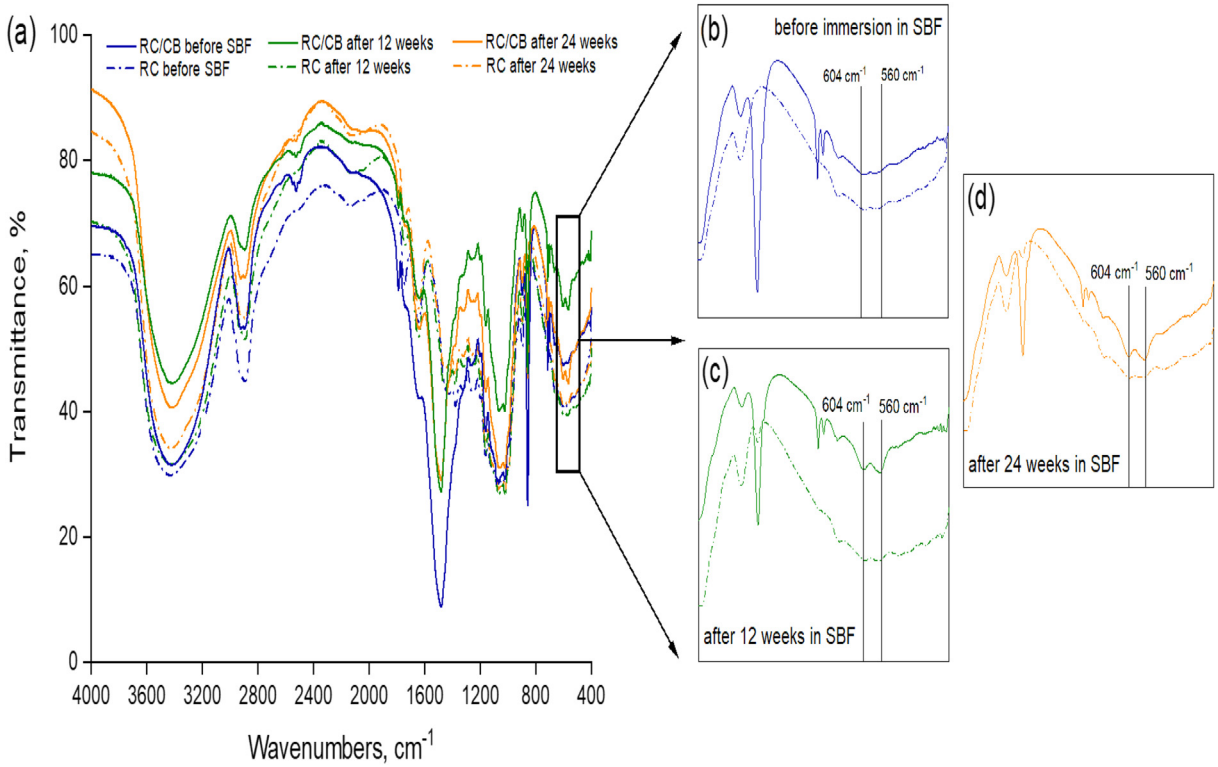

Fig. 4. FTIR spectra of the scaffolds during soaking in 1x SBF up to 24 weeks (a) and magnification of zones of interest: scaffolds before immersion in SBF (b); scaffolds after 12 weeks of immersion in SBF (c); scaffolds after 24 weeks of immersion in SBF (d). Spectra of the RC/CB scaffolds are presented as a solid line, spectra of the RC scaffolds are presented as a dash-dot line.

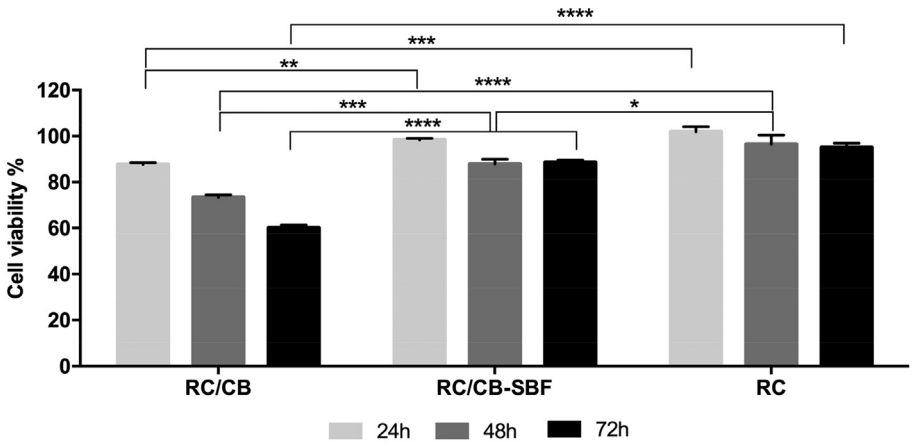

Fig. 5. The *in vitro* cell viability of MG-63 cells incubated with extracts of cellulose-based scaffolds for 24 h, 48 h and 72 h (a); MG-63 proliferation on cellulose-based scaffolds on the 14th day of incubation (b); ALP activity of MG-63 cells cultured on cellulose-based scaffolds for 7, 14 and 21 days (c).

scaffold surface. Additionally, 10x SBF coating on RC/CB scaffolds increased cell distribution on the surface.

Fluorescence imaging was performed to determine the cell-scaffold surface interaction. RC/CB (Fig. 6 (a, b, c)) and RC/CB-SBF scaffolds (Fig. 6 (d, e, f)) provided a favorable surface for cell attachment and proliferation compared to RC scaffold (Fig. 6 (g, h, i)). The results indicated that enhanced cell attachment was observed on cuttlebone-incorporated scaffolds. This result may arise from the chemical structure of cuttlebone, which consists of the ß-chitin structure. Kaya et al. [34] investigated the protein adsorption capacity of ß-chitin from cuttlebone and compared its activity to α-chitin from an insect. They revealed that ß-chitin had a higher bovine serum albumin adsorption capacity than α-allomorph.

Additionally, 10x SBF coating enhanced the cell attachment on RC/CB scaffolds. SBF solutions that lead to apatite calcium phosphate formation are known to increase the scaffold bioactivity by the calcium phosphate ions inducing re-deposition of carbonate apatite crystallites on the surface and proteins [35,36]. 10x SBF-coated PCL scaffolds were fabricated, and it was reported that immersion of scaffolds in the 10x SBF solution enhanced the cell distribution density [37].

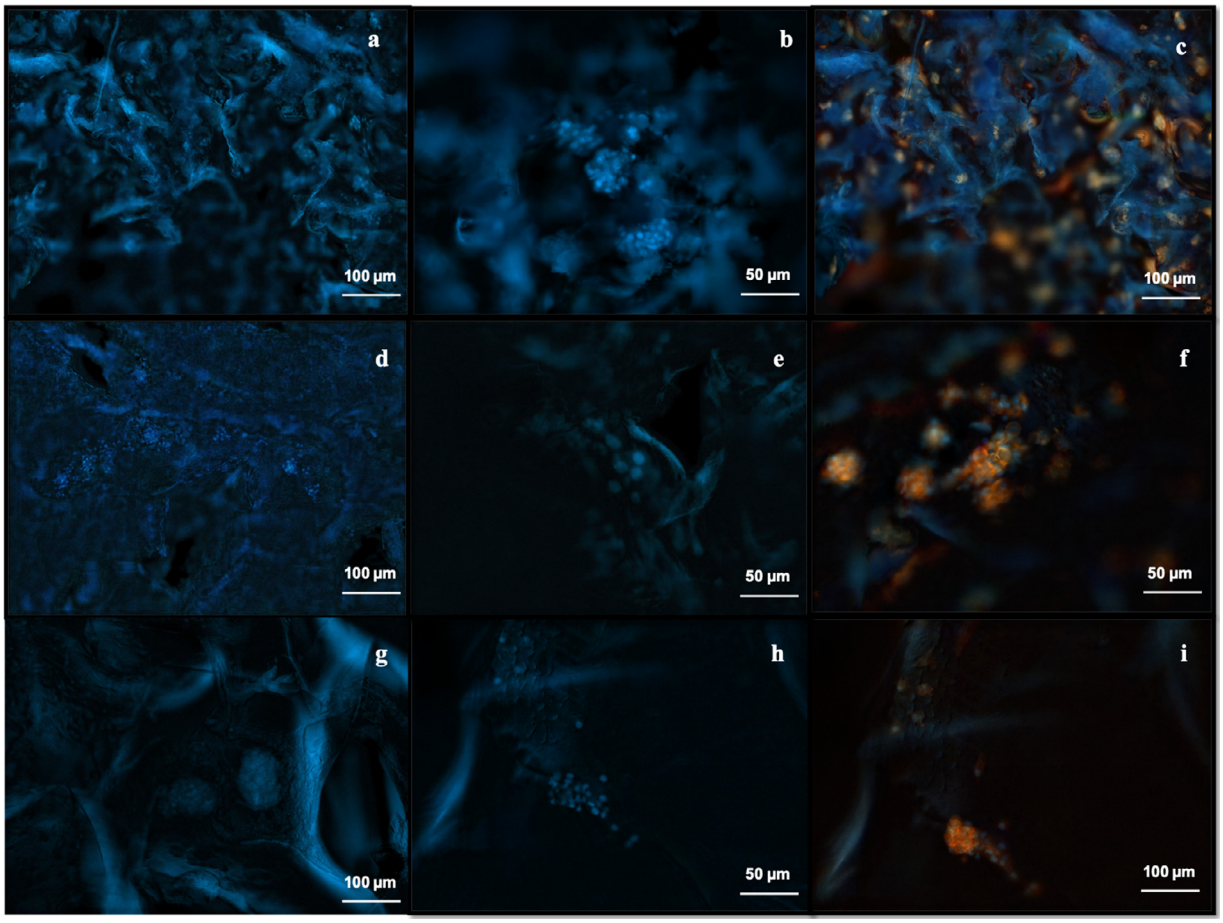

Fig. 6. Fluorescence images of MG-63 cells on cellulose-based scaffolds for 7 days (DAPI-Alexa Fluor 555): RC/CB (a, b, c); RC/CB-SBF (d, e, f); RC (g, h, i).

3.5. Cell proliferation assay

MG-63 cells were incubated on cellulose-based scaffolds for the 14th day of incubation to determine the effects of cuttlebone incorporation on osteoblast proliferation. MG-63 proliferation on cellulose-based scaffolds is depicted in Fig. 7 (a). The results showed that MG-63 cells proliferated successfully on scaffolds with an increasing trend. On the 7th day of incubation, the cell proliferation results of all cellulose-based scaffolds were found to be statistically significant compared to the control group (RC scaffold).

Cell proliferation data indicated that a distinct increase in cell proliferation was obtained for RC/CB and RC/CB-SBF scaffolds compared to the RC scaffolds. On the 14th day of incubation, the maximum cell proliferation was obtained on 10x SBF-coated RC/CB scaffolds. Thus, 10x SBF coating on a scaffold surface may lead to enhancing the effect on cell proliferation. Similarly, Choong and co-workers [38] revealed that PCL scaffolds covered with 1.5x SBF had higher proliferation rate compared to uncoated scaffolds. LDH assay results showed that cell death was lower at early incubation periods and there is an increase in LDH activity at the late incubation periods as the cell population increased on the scaffolds (Fig. 7 (b)). However, a similar trend was observed on RC/CB scaffolds compared to control group (RC). No significant difference was observed between groups at the 14th day of incubation.

3.6. Alkaline phosphatase activity

Osteogenic activity of MG-63 cells on scaffolds was evaluated by ALP activity determination (Fig. 7 (c)). ALP activity results showed that the highest ALP production was obtained on RC/CB scaffolds compared to the RC scaffold. No significant difference was obtained statistically between groups for all incubation periods. The ALP activity of MG-63 cells increased with incubation time as expected in early osteoblast differentiation. ALP activity levels of cells on scaffolds increased significantly from the 14th day of culture to the 21st day of culture, especially for the cells on the RC/CB-SBF scaffolds. The groups showed a significant increasing trend in ALP activity with respect to time. At each time point, no significant difference was observed between the groups.

ALP activity is the key factor that is known as a marker for osteogenic activity and osteoblast differentiation. In early bone formation, ALP expression of osteoblasts increases and leads to the initiation of calcification. In our study, MG-63 cells showed a similar ALP activity on RC/CB and RC/CB-SBF scaffolds. The results indicated that incorporation of cuttlebone did not show a considerable effect on ALP activity of MG-63 cells. However, MG-63 cells cultured on all scaffold groups expressed increasing ALP production according to incubation time. Choong and co-workers [38] also studied the effects of 1.5x SBF solution on the bioactivity of PCL scaffolds. The ALP assay results showed that the human bone marrow cells seeded on the coated scaffolds had higher ALP activity compared to the cells on uncoated scaffolds.

3.7. Osteocalcin secretion

Osteocalcin secretion of MG-63 cells on RC/CB scaffolds was depicted in Fig. 7 (d). Results showed that OC concentration on 10x SBF coated RC/CB scaffolds is higher compared to RC/CB scaffolds.

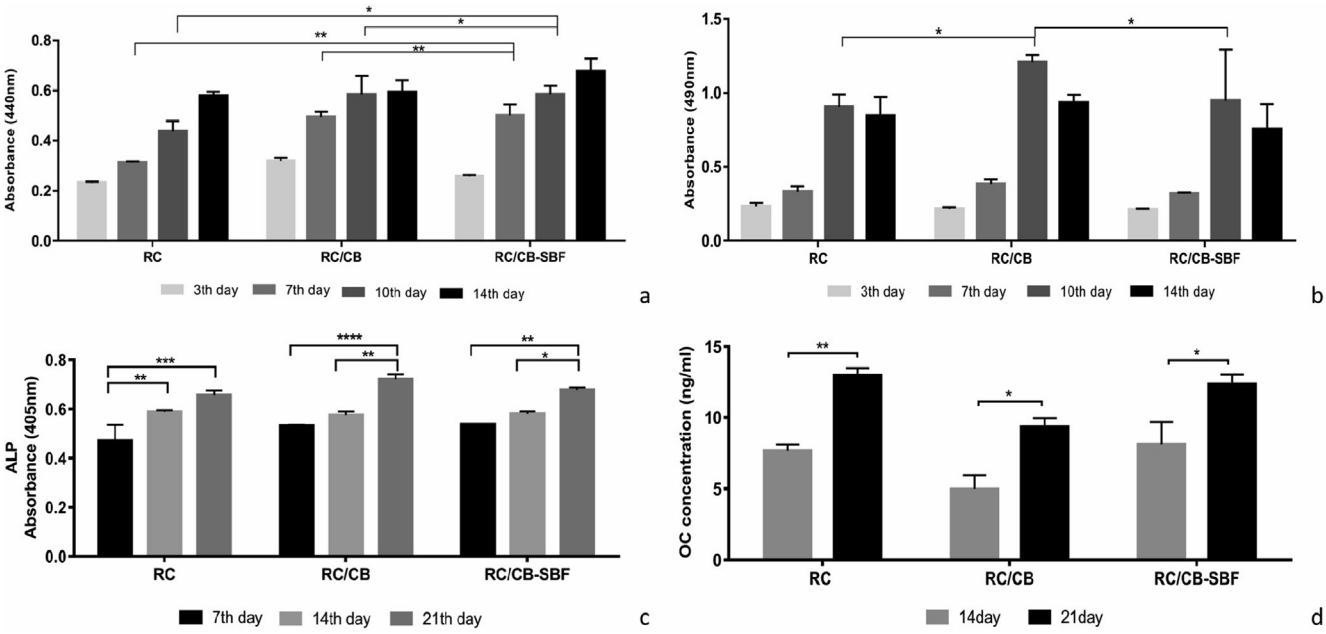

Fig. 7. MG-63 proliferation on scaffolds for 3, 7, 10 and 14 days of incubation (a); LDH activity for 3, 7, 10 and 14 days of incubation periods (b); ALP activity of MG-63 cells cultured on scaffolds for 7, 14 and 21 days (c); Osteocalcin concentration for 14 and 21 days (d).

3.8. In vitro biomineralization of MG-63 cells on scaffolds

Mineralization was determined by calcium and phosphate mineral deposition on the scaffolds qualitatively with von Kossa and Alizarin Red S staining protocols. Mineral deposition was observed in each group on the 7th day of incubation (Fig. 8). Higher calcium and phosphate depositions were prominently observed on cellulose-based composite scaffolds compared to the RC scaffold as a control group (Fig. 8 (e, f)). 10x SBF coating on RC/CB scaffolds (Fig. 8 (c, d)) enhanced the biomineralization on the surface compared to the control group.

The von Kossa staining method has been used to represent the "amount of calcification". Von Kossa stain does not react with calcium but reacts with phosphate in the presence of the acidic material. Thus, it actually detects phosphate deposition that is generally used for determination of "calcification" and bonelike mineral formation by cells. However, the presence of phosphate deposition does not necessarily imply the presence of calcium or HAp [39,40]. Therefore, biomineralization of MG-63 cells was evaluated by the Alizarin red staining method to verify the calcium deposition together with von Kossa staining.

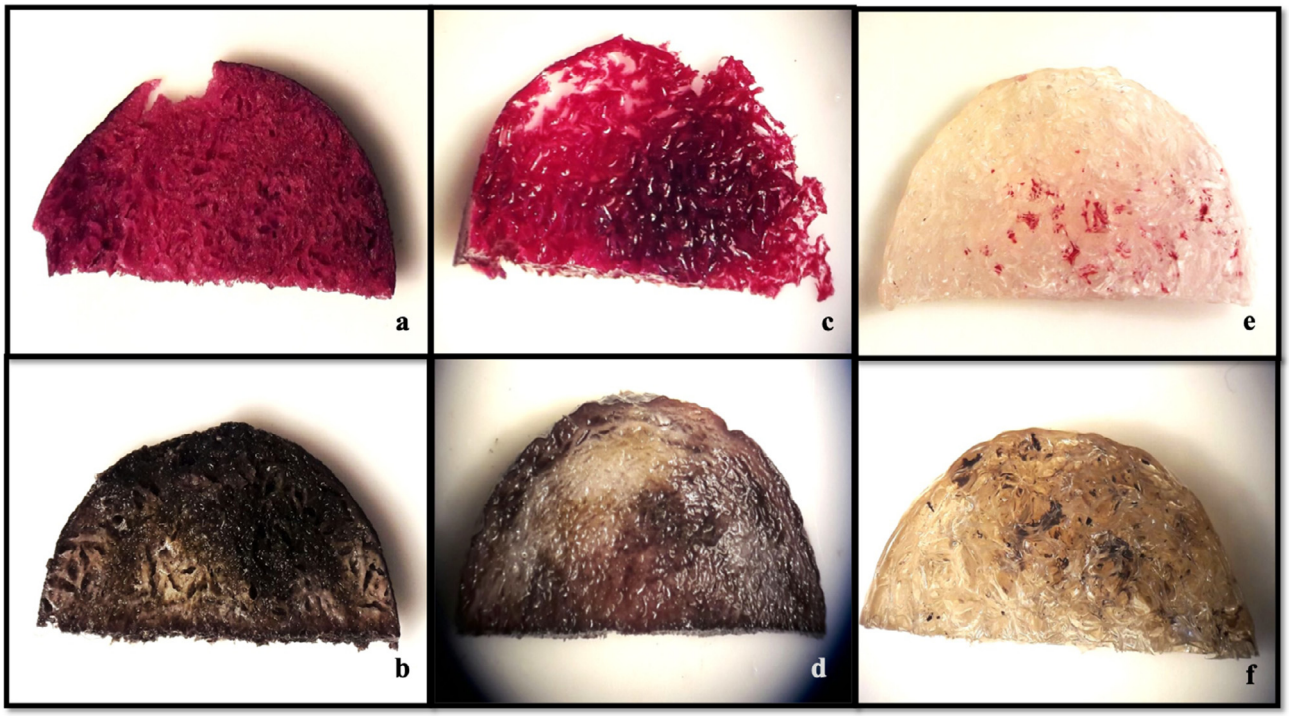

Fig. 8. Stereomicroscopy images of Alizarin red and von Kossa staining on RC/CB (a, b); RC/CB-SBF (c, d); and RC (e, f) scaffolds at 7 days.

Stereoimages indicated that, higher calcium and phosphate depositions were observed on cellulose-based composite scaffolds. The cuttlebone is a highly organized internal shell structure constructed from aragonite ($CaCO_3$) in association with a ß-chitin organic framework, which makes it particularly good for templating inorganic growth [41,42]. Therefore, cuttlebone incorporation to cellulose-based scaffolds improved mineral deposition capacity. In this study, the results showed that 10x SBF coating promoted the biomineralization of MG-63 cells on the RC/CB scaffold surface.

4. Conclusions

Continuing the research on cuttlebone and its application for the development of biomedical compositions, this study shows the impact of cuttlebone reinforcement and biomimetic coating on the osteoconductive properties of 3D porous cellulose-based scaffolds. Thermogravimetric analysis results showed that predominant portion of chitin (9%) is located in a dorsal segment of cuttlebone, while 5% of chitin is concentrated in a lamellar part. Soaking of the scaffolds in 1x simulated body fluid up to 24 weeks showed that the surface of cuttlebone-reinforced cellulose scaffolds was continuously covering with a compact layer of apatite precursor spheres, forming the aggregates by increasing the crystal size.

Biomimetic coating via immersion of cellulose/cuttlebone scaffolds in a concentrated 10x simulated body fluid promoted biomineralization of MG-63 cells on a surface of the scaffolds. The scaffold extracts of each group did not show any cytotoxic effect on MG-63 cell lines. Fluorescence microscopy images of MG-63 cells showed that cuttlebone incorporation promoted cell attachment on the cellulose/cuttlebone scaffolds, which could be explained by ß-chitin capacity to adsorb proteins.

To conclude, maximum effect for apatite nucleation and enhancing osteoconductive properties of the cellulose-based scaffolds was achieved following the two technological steps: 1st, by mixing cuttlebone with polymer gel during matrix formation and 2nd, via subsequent coating of the scaffold surface using concentrated 10x simulated body fluid. According to the results of the study, cellulose/cuttlebone scaffolds, subjected to biomimetic coating with 10x simulated body fluid elements, could be described as a promising candidate for bone tissue engineering applications.

Funding

This research did not receive any specific grant from funding agencies in the public, commercial, or not-for-profit sectors.

Acknowledgments

The authors thank Dr. Berivan Erik Cecen from Dokuz Eylul University Biomechanic Department for supplying the MG-63 cell line. The authors are grateful to the İzmir Institute of Technology Biotechnology and Bioengineering Research and Application Center (Iztech Biomer) for fluorescence microscopy analyses and the Center for Materials Research (Iztech CMR) for stereomicroscope imaging. The authors thank researcher Dr. Marina Sokolova from Rudolfs Cimdins Riga Biomaterial Innovations and Development Centre, Riga Technical University, for cuttlebone particle size analysis. The authors also thank multimedia specialist Lukas Motiejūnas from Kaunas University of Technology Department of Marketing for preparing the supplementary digital video.

Appendix A. Supplementary material

Supplementary data to this article can be found online at https://doi.org/10.1016/j.ijbiomac.2019.10.213.

References

[1] E. Dogan, Z. Okumus, Cuttlebone used as a bone xenograft in bone healing, Vet. Med-Czech. 59 (2014) 254–260.
[2] B.S. Kim, H.J. Kang, S.S. Yang, J. Lee, Comparison of in vitro and in vivo bioactivity: cuttlefish-bone-derived hydroxyapatite and synthetic hydroxyapatite granules as a bone graft substitute, Biomed. Mater. 9 (2014), https://doi.org/10.1088/1748-6041/9/2/025004 025004.
[3] M.G. Raucci, V. Guarino, L. Ambrosio, Biomimetic strategies for bone repair and regeneration, J. Funct. Biomater. 3 (2012) 688–705, https://doi.org/10.3390/jfb3030688.
[4] O. Petrauskaite, P.D.S. Gomes, M.H. Fernandes, G. Juodzbalys, A. Stumbras, J. Maminskas, L. Liesiene, M. Cicciù, Biomimetic mineralization on a macroporous cellulose-based matrix for bone regeneration, Biomed. Res. Int. 2013 (2013), https://doi.org/10.1155/2013/452750.
[5] K. Rezwan, Q.Z. Chen, J.J. Blaker, A.R. Boccaccini, Biodegradable and bioactive porous polymer/inorganic composite scaffolds for bone tissue engineering, Biomaterials 27 (2006) 3413–3431, https://doi.org/10.1016/j.biomaterials.2006.01.039.
[6] S. Saber-Samandari, K. Alamara, S. Saber-Samandari, Calcium phosphate coatings: Morphology, micro-structure and mechanical properties, Ceram. Int. 40 (2014) 563–572, https://doi.org/10.1016/j.ceramint.2013.06.038.
[7] A. Abdal-hay, K.A. Khalil, A.S. Hamdy, F.F. Al-Jassir, Fabrication of highly porous biodegradable biomimetic nanocomposite as advanced bone tissue scaffold, Arab. J. Chem. 10 (2017) 240–252, https://doi.org/10.1016/j.arabjc.2016.09.021.
[8] T.E.L. Douglas, G. Krawczyk, E. Pamula, H.A. Declercq, D. Schaubroeck, M.M. Bucko, L. Balcaen, P.V.D. Voort, V. Bliznuk, N.M.F. van den Vreken, M. Dash, R. Detsch, A.R. Boccaccini, F. Vanhaecke, M. Cornelissen, P. Dubruel, Generation of composites for bone tissue-engineering applications consisting of gellan gum hydrogels mineralized with calcium and magnesium phosphate phases by enzymatic means, J. Tissue Eng. Regen. Med. 10 (2016) 938–954, https://doi.org/10.1002/term.1875.
[9] C. He, X. Jin, P.X. Ma, Calcium phosphate deposition rate, structure and osteoconductivity on electrospun poly (L-lactic acid) matrix using electrodeposition or simulated body fluid incubation, Acta Biomater. 10 (2014) 419–427, https://doi.org/10.1016/j.actbio.2013.08.041.
[10] M.J. Lee, J.B. Park, H.H. Kim, C.S. Ki, S.Y. Park, H.J. Kim, Y.H. Park, Surface coating of hydroxyapatite on silk nanofiber through biomineralization using ten times concentrated simulated body fluid and the evaluation for bone regeneration, Macromol. Res. 22 (2014) 710–716, https://doi.org/10.1007/s13233-014-2114-x.
[11] S. Aday, M. Gümüşderelioğlu, Bone-like apatite-coated chitosan scaffolds: Characterization and osteoblastic activity, Polym. Compos. 31 (2010) 1418–1426, https://doi.org/10.1002/pc.20927.
[12] L. Kong, Y. Gao, G. Lu, Y. Gong, Z. Zhao, X. Zhang, A study on the bioactivity of chitosan/nano-hydroxyapatite composite scaffolds for bone tissue engineering, Eur. Polym. J. 42 (2006) 3171–3179, https://doi.org/10.1016/j.eurpolymj.2006.08.009.
[13] S. Saber-Samandari, S. Saber-Samandari, S. Kiyazar, J. Aghazadeh, A. Sadeghi, In vitro evaluation for apatite-forming ability of cellulose-based nanocomposite scaffolds for bone tissue engineering, Int. J. Biol. Macromol. 86 (2016) 434–442, https://doi.org/10.1016/j.ijbiomac.2016.01.102.
[14] P. Fonte, S. Reis, B. Sarmento, Facts and evidences on the lyophilization of polymeric nanoparticles for drug delivery, J. Controll. Release. 10 (2016) 75–86, https://doi.org/10.1016/j.jconrel.2016.01.034.
[15] A. Kordjamshidi, S. Saber-Samandari, M. Ghadiri Nejad, A. Khandan, Preparation of novel porous calcium silicate scaffold loaded by celecoxib drug using freeze drying technique: Fabrication, characterization and simulation, Ceram. Int. 45 (2019) 4126–14135, https://doi.org/10.1016/j.ceramint.2019.04.113.
[16] Z. Shahbazarab, A. Teimouri, A.N. Chermahini, M. Azadi, Fabrication and characterization of nanobiocomposite scaffold of zein/chitosan/nanohydroxyapatite prepared by freeze-drying method for bone tissue engineering, Int. J. Biol. Macromol. 108 (2018) 1017–1027, https://doi.org/10.1016/j.ijbiomac.2017.11.017.
[17] A. Palaveniene, V. Harkavenko, V. Kharchenko, P. Daugela, M. Pranskunas, G. Juodzbalys, J. Liesiene, Cuttlebone as a marine-derived material for preparing bone grafts, Mar. biotechnol. 20 (3) (2018) 363–374, https://doi.org/10.1007/s10126-018-9816-6.
[18] O. Petrauskaite, J. Liesiene, C. Santos, P.S. Gomes, M. Garcia, M.H. Fernandes, M. M. Almeida, M.E.V. Costa, G. Juodzbalys, P. Daugela, Nano-hydroxyapatite/cellulose composite scaffold for bone tissue engineering, J. Tissue Eng. Reg. Med. 6 (2012) 34-34.
[19] T. Kokubo, H. Kushitani, S. Sakka, T. Kitsugi, T. Yamamuro, Solutions able to reproduce in vivo surface-structure changes in bioactive glass-ceramic A-W3, J. Biomed. Mater. Res. 24 (1990) 721–734, https://doi.org/10.1002/jbm.820240607.
[20] M.V. Berridge, A.S. Tan, K.D. McCoy, R. Wang, The biochemical and cellular basis of cell proliferation assays that use tetrazolium salts, Biochemica. 4 (1996) 14–19.
[21] K. Periasamy, G.C. Mohankumar, Sea coral-derived cuttlebone reinforced epoxy composites: Characterization and tensile properties evaluation with mathematical models, J. Compos. Mater. 50 (2016) 807–823, https://doi.org/10.1177/0021998315581512.

[22] M. Florek, E. Fornal, P. Gómez-Romero, E. Zieba, W. Paszkowicz, J. Lekki, J. Nowak, A. Kuczumow, Complementary microstructural and chemical analyses of Sepia officinalis endoskeleton, Mater. Sci. Eng. C. 29 (2009) 1220–1226, https://doi.org/10.1016/j.msec.2008.09.040.
[23] P. Kamalbabu, G.M. Kumar, Effects of particle size on tensile properties of marine coral reinforced polymer composites, Proced. Mater. Sci. 5 (2014) 802–808, https://doi.org/10.1016/j.mspro.2014.07.331.
[24] C. Le Pabic, A. Marie, B. Marie, A. Percot, L. Bonnaud-Ponticelli, P.J. Lopez, G. Luquet, First proteomic analyses of the dorsal and ventral parts of the Sepia officinalis cuttlebone, J. Proteomics. 150 (2017) 63–73, https://doi.org/10.1016/j.jprot.2016.08.015.
[25] H. Alyami, E. Dahmash, J. Bowen, A.R. Mohammed, An investigation into the effects of excipient particle size, blending techniques and processing parameters on the homogeneity and content uniformity of a blend containing low-dose model drug, PloS one. 12 (2017), https://doi.org/10.1371/journal.pone.0178772 e0178772.
[26] A. Palavenienė, K. Glambaite, A. Jaskūnas, O. Baniukaitienė, J. Liesienė, Biomimetic mineralization on cellulose/cuttlebone scaffolds, Chemija. 28 (3) (2017) 148–153.
[27] C. Rey, C. Combes, C. Drouet, H. Sfihi, A. Barroug, Physico-chemical properties of nanocrystalline apatites: implications for biominerals and biomaterials, Mater. Sci. Eng. C. 27 (2007) 198–205, https://doi.org/10.1016/j.msec.2006.05.015.
[28] A.F. Brito, B. Antunes, F. dos Santos, H.R. Fernandes, J.M. Ferreira, Osteogenic capacity of alkali-free bioactive glasses. In vitro studies, J. Biomed. Mater. Res. B Appl. Biomater. 105 (2017) 2360–2365, https://doi.org/10.1002/jbm.b.33771.
[29] H. Deplaine, M. Lebourg, P. Ripalda, A. Vidaurre, P. Sanz-Ramos, G. Mora, F. Prósper, I. Ochoa, M. Doblaré, J.L. Gómez Ribelles, I. Izal-Azcárate, G. Gallego Ferrer, Biomimetic hydroxyapatite coating on pore walls improves osteointegration of poly(L-lactic acid) scaffolds, J. Biomed. Mater. Res. B Appl. Biomater. 101 (2013) 173–186, https://doi.org/10.1002/jbm.b.32831.
[30] Y.F. Chou, W.A. Chiou, Y. Xu, J.C. Dunn, B.M. Wu, The effect of pH on the structural evolution of accelerated biomimetic apatite, Biomaterials 25 (2004) 5323–5331, https://doi.org/10.1016/j.biomaterials.2003.12.037.
[31] L. Berzina-Cimdina, N. Borodajenko, Research of calcium phosphates using Fourier transform infrared spectroscopy Infrared Spectroscopy-Materials Science, Engineering and Technology, InTech (2012), https://doi.org/10.5772/36942.
[32] J.H. Pang, X. Liu, M. Wu, Y.Y. Wu, X.M. Zhang, R.C. Sun, Fabrication and characterization of regenerated cellulose films using different ionic liquids, J. Spectro. (2014), https://doi.org/10.1155/2014/214057.
[33] X. Li, Y. Zhao, Y. Bing, Y. Li, N. Gan, Z. Guo, Z. Peng, Y. Zhu, Biotemplated syntheses of macroporous materials for bone tissue engineering scaffolds and experiments in vitro and vivo, ACS Appl. Mater. Interfaces 5 (2013) 5557–5562, https://doi.org/10.1021/am400779e.
[34] M. Kaya, I. Sargin, V. Aylanc, M.N. Tomruk, S. Gevrek, I. Karatoprak, N. Colak, Y. G. Sak, E. Bulut, Comparison of bovine serum albumin adsorption capacities of α-chitin isolated from an insect and β-chitin from cuttlebone, J. Ind. Eng. Chem. 38 (2016) 146–156, https://doi.org/10.1016/j.jiec.2016.04.015.
[35] M. Neo, S. Kotani, T. Nakamura, T. Yamamuro, C. Ohtsuki, T. Kokubo, Y. Bando, A comparative study of ultrastructures of the interfaces between four kinds of surface-active ceramic and bone, J. Biomed. Mater. Res. 26 (1992) 1419–1432, https://doi.org/10.1002/jbm.820261103.
[36] F.B. Bagambisa, U. Joos, W. Schilli, Mechanisms and structure of the bond between bone and hydroxyapatite ceramics, J. Biomed. Mater. Res. 27 (1993) 1047–1055, https://doi.org/10.1002/jbm.820270810.
[37] I.G. Beşkardeş, M. Gümüşderelioğlu, Biomimetic apatite-coated PCL scaffolds: effect of surface nanotopography on cellular functions, J. Bioact/ Compat. Polym. 24 (2009) 507–524, https://doi.org/10.1177/0883911509349311.
[38] C. Choong, J.T. Triffitt, Z.F. Cui, Polycaprolactone scaffolds for bone tissue engineering: effects of a calcium phosphate coating layer on osteogenic cells, Food Bioprod. Process. 82 (2004) 117–125, https://doi.org/10.1205/0960308041614864.
[39] S.N. Meloan, H. Puchtler, Chemical mechanisms of staining methods: von Kossa's technique: what von Kossa really wrote and a modified reaction for selective demonstration of inorganic phosphates, J. Histotechnol. 8 (1985) 11–13, https://doi.org/10.1179/his.1985.8.1.11.
[40] L.F. Bonewald, S.E. Harris, J. Rosser, M.R. Dallas, S.L. Dallas, N.P. Camacho, B. Boyan, A. Boskey, von Kossa staining alone is not sufficient to confirm that mineralization in vitro represents bone formation, Calcif. Tissue Int. 72 (2003) 537–547, https://doi.org/10.1007/s00223-002-1057-y.
[41] J.D. Birchall, N.L. Thomas, On the architecture and function of cuttlefish bone, J. Mater. Sci. 18 (1983) 2081–2086, https://doi.org/10.1007/BF00555001.
[42] W. Ogasawara, W. Shenton, S.A. Davis, S. Mann, Template mineralization of ordered macroporous chitin–silica composites using a cuttlebone-derived organic matrix, Chem. Mat. 12 (2000) 2835–2837, https://doi.org/10.1021/cm0004376.